Atmospheric Concentrations of Greenhouse Gases

Identification

1. Indicator Description

This indicator describes how the levels of major greenhouse gases (GHGs) in the atmosphere have changed over geological time and in recent years. Changes in atmospheric GHGs, in part caused by human activities, affect the amount of energy held in the Earth-atmosphere system and thus affect the Earth's climate. This indicator is highly relevant to climate change because greenhouse gases from human activities are the primary driver of observed climate change since the mid-20th century (IPCC, 2021).

Components of this indicator include:

- Global atmospheric concentrations of carbon dioxide over time (Figure 1).
- Global atmospheric concentrations of methane over time (Figure 2).
- Global atmospheric concentrations of nitrous oxide over time (Figure 3).
- Global atmospheric concentrations of selected halogenated gases over time (Figure 4).
- Global atmospheric concentrations of ozone over time (Figure 5).

2. Revision History

April 2010:	Indicator published.
December 2012:	Updated indicator with data through 2011. Added nitrogen trifluoride to Figure 4.
August 2013:	Updated indicator with data through 2012.
May 2014:	Updated Figures 1, 2, and 3 with data through 2013, and Figure 4 with data through 2012. Added Figure 5 to show trends in ozone.
June 2015:	Updated Figures 1, 2, and 3 with data through 2014.
April 2016:	Updated Figure 1 with data through 2015.
August 2016:	Updated Figures 2, 3, and 4 with data through 2015; updated Figure 5 with data through 2014.
April 2021:	Updated Figures 1, 2, and 3 with data through 2019; updated Figures 4 and 5 with data through 2018.
July 2022:	Updated Figures 1, 2, 3, and 4 with data through 2021; updated Figure 5 with data through 2020.
June 2024:	Updated Figures 1, 2, and 3 with data through 2023; updated Figure 4 with data through 2022.

Data Sources

3. Data Sources

Ambient concentration data used to develop this indicator were taken from the following sources:

Figure 1. Global Atmospheric Concentrations of Carbon Dioxide Over Time

- Antarctic ice cores: approximately 803,719 BCE to 2001 CE—Bereiter et al. (2015). This is a composite of the following individual sources (see Bereiter et al., 2015, for corresponding full citations):
  - Law Dome (Rubino et al., 2013)
  - Law Dome (MacFarling Meure et al., 2006)
  - Dome C (Monnin et al., 2001, 2004)
  - WAIS (Marcott et al., 2014) minus 4 parts per million by volume
  - Siple Dome (Ahn et al., 2014)
  - TALDICE (Bereiter et al., 2012)
  - EDML (Bereiter et al., 2012)
  - Dome C Sublimation (Schneider et al., 2013)
  - Vostok (Petit et al., 1999)
  - Dome C (Siegenthaler et al., 2005)
  - Dome C (Bereiter et al., 2014)
- Mauna Loa, Hawai‘i: 1959 CE to 2023 CE—NOAA (2024a).
- Barrow (Utqiaġvik), Alaska: 1974 CE to 2023 CE; Cape Matatula, American Samoa: 1976 CE to 2023 CE; South Pole, Antarctica: 1976 CE to 2023 CE—NOAA (2024b).
- Cape Grim, Australia: 1977 CE to 2023 CE—CSIRO (2024a).
- Shetland Islands, Scotland: 1993 CE to 2002 CE—Steele et al. (2007).
- Lampedusa Island, Italy: 1993 CE to 2000 CE—Chamard et al. (2001).

Figure 2. Global Atmospheric Concentrations of Methane Over Time

- EPICA Dome C, Antarctica: approximately 797,446 BCE to 1937 CE—Loulergue et al. (2008).
- Law Dome, Antarctica: approximately 1008 CE to 1980 CE—Etheridge et al. (2002).
- Cape Grim, Australia: 1985 CE to 2023 CE—CSIRO (2024b).
- Mauna Loa, Hawai‘i: 1984 CE to 2022 CE—NOAA (2023b).
- Shetland Islands, Scotland: 1993 CE to 2001 CE—Steele et al. (2002).

Figure 3. Global Atmospheric Concentrations of Nitrous Oxide Over Time

- EPICA Dome C, Antarctica: approximately 796,475 BCE to 1937 CE—Schilt et al. (2010).
- Antarctica: approximately 1903 CE to 1979 CE—Battle et al. (1996).
- Cape Grim, Australia: 1979 CE to 2022 CE—CSIRO (2024c), supplemented with some historical gap-filling data from NOAA (https://gaw.kishou.go.jp/search/file/0002-5011-1003-01-02-3004) and AGAGE (https://gaw.kishou.go.jp/search/file/0004-5011-1003-01-01-2001 and https://gaw.kishou.go.jp/search/file/0004-5011-1003-01-01-2011).
- South Pole, Antarctica: 1998 CE to 2023 CE; Barrow (Utqiaġvik), Alaska: 1999 CE to 2023 CE—NOAA (2024c).
- Mauna Loa, Hawai‘i: 2000 CE to 2021 CE—NOAA (2023c).

Figure 4. Global Atmospheric Concentrations of Selected Halogenated Gases, 1978–2022

Global average atmospheric concentration data for selected halogenated gases were obtained mainly from the Advanced Global Atmospheric Gases Experiment (AGAGE, 2022), and from NOAA via Stephen Montzka (NOAA, 2023a). These data set contributions were as follows:

- AGAGE (2022) for halon-1211 for February 1992–December 2003; HCFC-22, HCFC-141b, HFC-125, HFC-152a, and halon-1211 for January 2004–March 2021; HFC-23 for October 2007–March 2021; HFC-134a for January 2003–March 2021; methyl chloroform, sulfur hexafluoride, and PFC-116 for January 2004–February 2022; nitrogen trifluoride for February 2015–March 2021; and PFC-14 for May 2006–March 2021.

- NOAA (2023a) for HCFC-22, HCFC-141b, HFC-125, HFC-134a, HFC-152a, and halon-1211 for April 2021–December 2022; CFC-12 for April 2020–December 2022; and methyl chloroform for April 2022–December 2022.

Historical data for some species, whose time series could be extended by including data from other studies, were obtained from these sources:

- AGAGE (2021) for CFC-12 for July 1989–March 2020; and methyl chloroform for July 1978–December 2003.

- Rigby (2017) for nitrogen trifluoride data before February 2015 and PFC-14 data before April 2006.

- Historical data provided by Dr. Ray Wang of AGAGE, representing AGAGE-approved data that predate the period currently available for download on the AGAGE website for HCFC-22, HCFC-141b, HFC-125, HFC-134a, HFC-152a, and sulfur hexafluoride for 2003 and earlier; CFC-12 before July 1978; and HFC-23 for 2004 and earlier (AGAGE, 2011).

A similar figure based on AGAGE and NOAA data appears in the Intergovernmental Panel on Climate Change's (IPCC's) Fifth Assessment Report (see Figure 2.4 in IPCC, 2013).

Figure 5. Global Atmospheric Concentrations of Ozone, 1979–2020
Ozone data were obtained from several National Aeronautics and Space Administration (NASA) sources:

- The Solar Backscatter Ultraviolet (SBUV) merged ozone data set (NASA, 2022) for total ozone.

- The Tropospheric Ozone Residual (TOR) (NASA, 2013) and Ozone Monitoring Instrument (OMI) Level 2 (NASA, 2021) data sets for tropospheric ozone.

4. Data Availability

The data used to develop Figures 1, 2, 3, and 5 of this indicator are publicly available and can be accessed from the references listed in Section 3. There are no known confidentiality issues.

The data set used for nitrous oxide in Antarctica in Exhibit 3 from Battle et al. (1996) has been subsumed within a newer set available at: https://daac.ornl.gov/cgi-bin/dsviewer.pl?ds_id=797.

Data for all of the halogenated gases in Figure 4 were downloaded from the AGAGE website at: https://agage2.eas.gatech.edu/data_archive/global_mean, which presented data through the end of

2021, and provided in spreadsheet form by Dr. Stephen Montzka of NOAA with data through the end of 2022 (NOAA, 2023a). Additional AGAGE data for PFC-14 and nitrogen trifluoride are also available at: https://agage2.eas.gatech.edu/data_archive/global_mean and were published in June 2021 (AGAGE, 2021). Additional historical monthly data for some of these gases were provided in spreadsheet form by Dr. Ray Wang of the AGAGE project team (AGAGE, 2011). NOAA's website (https://gml.noaa.gov/hats) also provides access to the global averages that are shown in Figure 4. Historical data for nitrogen trifluoride are based on measurements that were originally published in Arnold et al. (2013) and subsequently updated by the lead author and other collaborators. Historical PFC-14 and nitrogen trifluoride data were provided in spreadsheet form by Matthew Rigby of the University of Bristol.

Methodology

5. Data Collection

This indicator shows trends in atmospheric concentrations of several major GHGs that enter the atmosphere at least in part because of human activities: carbon dioxide (CO_2), methane (CH_4), nitrous oxide (N_2O), selected halogenated gases, and ozone.

Figures 1, 2, 3, and 4. Global Atmospheric Concentrations of Carbon Dioxide, Methane, Nitrous Oxide, and Selected Halogenated Gases Over Time

Figures 1, 2, 3, and 4 aggregate comparable, high-quality data from individual studies that each focused on different locations and time frames. Data since the mid-20th century come from global networks that use standard monitoring techniques to measure the concentrations of gases in the atmosphere. Older measurements of atmospheric concentrations come from ice cores—specifically, measurements of gas concentrations in air bubbles that were trapped in ice at the time the ice was formed. Scientists have spent years developing and refining methods of measuring gases in ice cores as well as methods of dating the corresponding layers of ice to determine their age. Ice core measurements are a widely used method of reconstructing the composition of the atmosphere before the advent of direct monitoring techniques.

This indicator presents a compilation of data generated by numerous sampling programs. The citations listed in Section 3 describe the specific approaches taken by each program. Gases are measured by mole fraction relative to dry air.

CO_2, CH_4, N_2O, and most of the halogenated gases presented in this indicator are considered to be well-mixed globally, due in large part to their long residence times in the atmosphere. Thus, while measurements over geological time tend to be available only for regions where ice cores can be collected (e.g., the Arctic and Antarctic regions), these measurements are believed to adequately represent concentrations worldwide. Recent monitoring data have been collected from a greater variety of locations, and the results show that concentrations and trends are indeed very similar throughout the world, although relatively small variations can be apparent across different locations.

Most of the gases shown in Figure 4 have been measured around the world numerous times per year. One exception is nitrogen trifluoride, which is an emerging gas of concern for which measurements have only recently started to become more widespread. The curve for nitrogen trifluoride in Figure 4 is based on samples collected in Australia and California through 2010, plus samples collected approximately monthly in California since 2010 and at additional sites in the most recent years. Measurements of air

samples collected before the mid-1990s are included in the data set, but they do not appear in Figure 4 because they are below the minimum concentration shown on the y-axis.

Nitrogen trifluoride was measured by the Medusa gas chromatography with mass spectrometry (GCMS) system, with refinements described in Weiss et al. (2008), Arnold et al. (2012), and Arnold et al. (2013). Mole fractions of the other halogenated gases were collected by AGAGE's Medusa GCMS system or similar methods employed by NOAA.

Figure 5. Global Atmospheric Concentrations of Ozone, 1979–2020

Unlike the gases in Figures 1, 2, 3, and 4, which are measured as atmospheric concentrations near ground level, Figure 5 describes the total "thickness" of ozone in the Earth's atmosphere. This measurement is called total column ozone, and it is typically measured in Dobson units. One Dobson unit represents a layer of gas that would be 10 micrometers (µm) thick under standard temperature and pressure (0°C/32°F and 0.987 atmospheres of air pressure).

Atmospheric ozone concentrations for this indicator are based on measurements by three sets of satellite instruments:

- **SBUV.** The SBUV observing system consists of a series of instruments aboard nine satellites that have collectively covered the period from 1970 to present, except for a gap from 1972 to 1978. SBUV measures the total ozone profile from the Earth's surface to the upper edge of the atmosphere (total column ozone) by analyzing solar backscatter radiation, which is the visible light and ultraviolet radiation that the Earth's atmosphere reflects back to space. This instrument can be used to determine the amount of ozone in each of 21 discrete layers of the atmosphere, which are then added together to get total column ozone. For a table of specific SBUV satellite instruments and the time periods they cover, see: https://acd-ext.gsfc.nasa.gov/Data_services/merged/instruments.html. A new instrument, the Ozone Mapping Profiler Suite (OMPS) Nadir Profiler, will continue the SBUV series. Although instrument design has improved over time, the basic principles of the measurement technique and processing algorithm remain the same, lending consistency to the record. For more information about the SBUV data set and how it was collected, see McPeters et al. (2013) and the references listed at: https://acd-ext.gsfc.nasa.gov/Data_services/merged/index.html.

- **Total Ozone Mapping Spectrometer (TOMS).** TOMS instruments have flown on four satellite missions that collectively cover the period from 1978 to 2005, with the exception of a period from late 1994 to early 1996 when no TOMS instrument was in orbit. Like SBUV, TOMS measured total ozone in the Earth's atmosphere by analyzing solar backscatter radiation. For more information about TOMS missions and instrumentation, see: https://eospso.nasa.gov/missions/total-ozone-mapping-spectrometer-earth-probe.

- **Aura OMI and Microwave Limb Sounder (MLS)**. The Aura satellite was launched in 2004, and its instruments (including OMI and MLS) were still collecting data as of February 13, 2024. The OMI instrument measures total column ozone by analyzing solar backscatter radiation. In contrast, the MLS measures emissions of microwave radiation from the Earth's atmosphere. This method allows the MLS to characterize the temperature and composition of specific layers of the atmosphere, including the amount of ozone within the stratosphere. To learn more about the

Aura mission and its instruments, visit: https://aura.gsfc.nasa.gov and: https://aura.gsfc.nasa.gov/scinst.html.

The instruments described above have flown on polar-orbiting satellites, which collect measurements that cover the entire surface of the Earth. For reasons of accuracy described in Section 9, however, this indicator is limited to data collected between 50°N and 50°S latitude. Solar backscatter measurements are restricted to daytime, when the sun is shining on a particular part of the Earth and not too low in the sky (i.e., avoiding measurements near sunrise or sunset).

6. Indicator Derivation

EPA obtained and compiled data from various GHG measurement programs and plotted these data in graphs. No attempt was made to project concentrations backward before the beginning of the ice core record (or the start of monitoring, in the case of Figures 4 and 5) or forward into the future.

Figures 1, 2, and 3. Global Atmospheric Concentrations of Carbon Dioxide, Methane, and Nitrous Oxide Over Time

Figures 1, 2, and 3 plot data at annual or multi-year intervals; with ice cores, consecutive data points are often spaced many years apart. EPA used the data exactly as reported by the organizations that collected them, with the following exceptions:

- Some of the recent time series for CO_2, CH_4, and N_2O consisted of monthly measurements. EPA averaged these monthly measurements to arrive at annual values to plot in the graphs. A few years did not have data for all 12 months. If at least 10 months of data were present in a given year, EPA averaged the available data to arrive at an annual value. If fewer than 10 monthly measurements were available, that year was excluded from the graph.
- Some ice core records were reported in terms of the age of the sample or the number of years before present. EPA converted these dates into calendar years.
- A few ice core records had multiple values at the same point in time (i.e., two or more different measurements for the same year, when the source lists years only as integers). These values were generally comparable and never varied by more than 4.8 percent. In such cases, EPA averaged the values to arrive at a single atmospheric concentration per year.

Figures 1, 2, and 3 present a separate line for each data series or location where measurements were collected. No methods were used to portray data for locations other than where measurements were made. The indicator does imply, however, that the values in the graphs represent global atmospheric concentrations—an appropriate assumption because the gases covered by this indicator have long residence times in the atmosphere and are considered to be well-mixed. In the indicator text, the key points refer to the concentration for the most recent year available. If data were available for more than one location, the text refers to the average concentration across these locations.

Figure 4. Global Atmospheric Concentrations of Selected Halogenated Gases, 1978–2022

Figure 4 plots data at sub-annual intervals (i.e., several data points per year). EPA used the data exactly as reported by the organizations that collected them. Figure 4 presents one trend line for each

halogenated gas, and these lines represent average concentrations across all measurement sites worldwide. These data represent monthly average mole fractions for each species, with the following exceptions: for halon-1211, HCFC-22, HCFC-141, HFC-125, HFC-134a, and HFC-152a, 2021 data are available for eight months and 2022 data are available for six months; for CFC-12 and methyl chloroform, 2020 data are available for eight months and 2021–2022 data are available for six months; halon-1211 data are only available at two-month intervals for data before January 2004, and nitrogen trifluoride measurements were converted into global annual average mole fractions using a model described in Arnold et al. (2013). The 2014 update of nitrogen trifluoride represented a change from the version of this indicator that EPA initially published in December 2012. At the time of the December 2012 version, modeled global annual average mole fractions had not yet been published in the literature, so EPA's indicator instead relied upon individual measurements of nitrogen trifluoride that were limited to the Northern Hemisphere.

EPA's 2021 web update represented a change from previous versions of this indicator by showing data from the AGAGE project for all the gas species presented. Previous versions presented data from other sources for all years of halon-1211, nitrogen trifluoride, and PFC-14. Beginning with the 2021 update, this indicator presents AGAGE data for all newly updated values while preserving the historical data values presented in previous versions of the indicator. Those historical values predate some species' inclusion in the AGAGE data set. In the case of all three gases, this switch resulted in the replacement of values shown in previous versions of this indicator for dates that overlapped with newly obtained data from AGAGE. In 2024, several gases were updated with data provided by NOAA through 2022. When NOAA and AGAGE data sets overlapped, the data set with the more recent publication date was used.

Data are available for additional halogenated species, but to make the most efficient use of the space available, EPA selected a subset of gases that are relatively common, have several years of data available, show marked growth trends (either positive or negative), and/or collectively represent most of the major categories of halogenated gases. The inclusion of nitrogen trifluoride here is based on several factors; like perfluoromethane (PFC-14 or CF_4), perfluoroethane (PFC-116 or C_2F_6), and sulfur hexafluoride, nitrogen trifluoride is a widely produced, fully fluorinated gas with a very high 100-year global warming potential (17,200) and a long atmospheric lifetime (740 years). Nitrogen trifluoride has experienced a rapid increase in emissions (i.e., more than 10 percent per year) due to its use in manufacturing semiconductors, flat screen displays, and thin film solar cells. Manufacturers started to replace perfluoroethane with nitrogen trifluoride in the electronics industry in the late 1990s.

To examine the possible influence of phase-out and substitution activities under the Montreal Protocol on Substances That Deplete the Ozone Layer, EPA divided Figure 4 into two panels: one for substances officially designated as "ozone-depleting" and one for all other halogenated gases.

Figure 5. Global Atmospheric Concentrations of Ozone, 1979–2020

NASA converted the satellite measurements into meaningful data products using the following methods:

- Data from all SBUV instruments were processed using the Version 8.6 algorithm (Bhartia et al., 2012; Kramarova, Frith, et al., 2013). The resulting data set indicates the amount of ozone in each of 21 distinct atmospheric layers, in Dobson units.

- NASA developed the TOR data set, which represents ozone in the troposphere only. They did so by starting with total column ozone measurements from TOMS and SBUV, then subtracting the

portion that could be attributed to the stratosphere. NASA developed this method using information about the height of the tropopause (the boundary between the troposphere and the stratosphere) over time and space, stratosphere-only ozone measurements from the Stratospheric Aerosol and Gas Experiment (SAGE) instrument that flew on some of the same satellites as TOMS, analysis of larger-scale patterns in stratospheric ozone distribution, and empirical corrections based on field studies. These methods are described in detail at: https://science-data.larc.nasa.gov/TOR/data.html and in Fishman et al. (2003) and the references cited therein.

- NASA developed the OMI Level 2 tropospheric ozone data set by essentially subtracting MLS stratospheric ozone observations from concurrent OMI total column ozone observations. Ziemke et al. (2006) describe these methods in more detail.

EPA performed the following additional processing steps to convert NASA's data products into an easy-to-understand indicator:

- EPA obtained SBUV data in the form of monthly averages for each layer of the atmosphere (total: 21 layers) by latitude band (i.e., average ozone levels for each 5-degree band of latitude). For each latitude band, EPA added the ozone levels for NASA's 21 atmospheric layers together to get total column ozone. Next, because each latitude band represents a different amount of surface area of the atmosphere (for example, the band near the North Pole from 85°N to 90°N covers a much smaller surface area than the band near the equator from 0° to 5°N), EPA calculated a global average using cosine area weighting. The global average in this indicator only covers the latitude bands between 50°N and 50°S for consistency of satellite coverage. EPA then combined the monthly averages to obtain annual averages.

- EPA obtained TOR and OMI Level 2 data as a grid of monthly average tropospheric ozone levels. Both data sets are divided into grid cells measuring 1 degree latitude by 1.25 degrees longitude and are only available between 50°N and 50°S. EPA calculated global monthly averages for each 1-degree latitude band by averaging over all grid cells in that band, then used cosine area weighting to calculate an average for the entire range from 50°N to 50°S. EPA combined the monthly averages to obtain annual averages.

In Figure 5, the "total column" line comes from the SBUV data set. Because of missing data from mid-1972 through late 1978, EPA elected to start the graph at 1979. From 1979 to present, all years have complete SBUV data.

The "troposphere" line in Figure 5 is based on the TOR data set from 1979 to 2004, the OMI Level 2 data set from 2006 to present, and an average of TOR and OMI Level 2 data for 2005. To correct for differences between the two instruments, EPA adjusted all OMI data points upward by 1.799 Dobson units, which is the documented difference during periods of overlap in 2004. This is a standard bootstrapping approach. Data are not shown from 1994 to 1996 because no TOMS instrument was in orbit from late 1994 to early 1996, so it was not possible to calculate annual averages from the TOR data set during these three years. The "stratosphere" line in Figure 5 was calculated by subtracting the "troposphere" series from the "total column" series.

Indicator Development

Figures 1, 2, 3, and 4 were first published as part of EPA's 2010 and 2012 climate change indicator reports. EPA added Figure 5 for the 2014 edition to address one of the key limitations of the previous indicator and to reflect the scientific community's growing awareness of the importance of tropospheric ozone as a contributor to climate change.

Scientists measure the amount of ozone in the atmosphere using two complementary methods. In addition to NASA's satellite-based data collection, NOAA operates a set of ground-based sites using devices called Dobson ozone spectrophotometers, which point upward and measure total column ozone on clear days. A set of 10 of these sites constitute the NOAA Ozone Reference Network. Measurements have been collected at some of these sites since the 1920s, and the resulting data are available at: www.esrl.noaa.gov/gmd/ozwv/dobson.

When developing this indicator, EPA chose to focus on satellite measurements because they allow total column ozone to be separated into tropospheric and stratospheric components, which facilitates greater understanding of the complex roles that ozone, ozone-depleting substances, and emissions of ozone precursors play in climate change. In addition to the fact that satellite-based data products were readily available to assess ozone concentrations by layer of the atmosphere, tropospheric ozone is short-lived and not globally mixed, so satellite-based measurements arguably provide more complete coverage of this greenhouse gas than a finite set of ground-based stations. Nonetheless, as described in Section 7, NOAA's ground-based measurements still play an important role in this indicator because they provide independent verification of the trends detected by satellites.

7. Quality Assurance and Quality Control

The data for this indicator have generally been taken from carefully constructed, peer-reviewed studies. Quality assurance and quality control procedures are addressed in the individual studies, which are cited in Section 3. Additional documentation of these procedures can be obtained by consulting with the principal investigators who developed each of the data sets.

NASA selected SBUV data for the official merged ozone data set based on the results of a detailed analysis of instrumental uncertainties (Deland et al., 2012) and comparisons against independent satellite and ground-based profile observations (Kramarova, Frith, et al., 2013; Labow et al., 2013). NASA screened SBUV data using the following rules:

- Data from the SBUV/2 instrument on the NOAA-9 satellite are not included due to multiple instrumental issues (Deland et al., 2012).
- Only measurements made between 8 AM and 4 PM Equatorial Crossing Time are included in the merged satellite ozone data set, with one exception in 1994–1995, when NOAA 11 data were included to avoid a gap in the data.
- When data from more than one SBUV instrument are available, NASA used a simple average of the data.
- Data were filtered for aerosol contamination after the eruptions of El Chichon (1982) and Mt. Pinatubo (1991).

Satellite data have been validated against ground-based measurements from NOAA's Ozone Reference Network. Figure TD-1 below shows how closely these two complementary data sources track each other over time.

Figure TD-1. Yearly Average Change in Global Total Column Ozone Since 1979

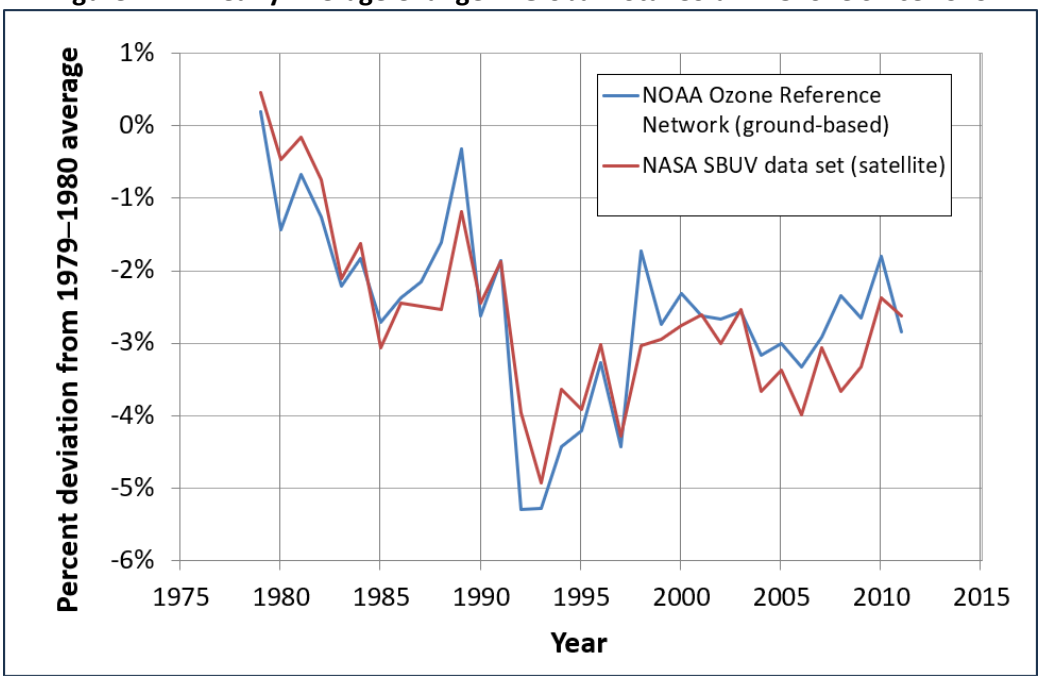

Analysis

8. Comparability Over Time and Space

Data have been collected using a variety of methods over time and space, but these methodological differences are expected to have little bearing on the overall conclusions for this indicator. The concordance of trends among multiple data sets collected using different program designs provides some assurance that the trends depicted actually represent changes in atmospheric conditions, rather than an artifact of sampling design.

Figures 1, 2, 3, and 4. Global Atmospheric Concentrations of Carbon Dioxide, Methane, Nitrous Oxide, and Selected Halogenated Gases

The gases covered in Figures 1, 2, 3, and 4 are all long-lived GHGs that are relatively evenly distributed globally. Thus, measurements collected at one particular location have been shown to be representative of average concentrations worldwide. Three gas species have measurements from more than one data source that have been combined into a single line on the graph (halon-1211, nitrogen trifluoride, and PFC-14). The switch from one data source to another occurs at a different time for each of the three species. In the case of halon-1211, the transition also represents a change from bimonthly to monthly measurements. A comparison of data where there was temporal overlap of readings between AGAGE (2022) and NOAA (2023a) or Rigby (2017) indicated that differences were within 2 percent on average between the sources.

Figure 5. Global Atmospheric Concentrations of Ozone, 1979–2020

Because ozone concentrations vary over time and space, Figure 5 uses data from satellites that cover virtually the entire globe, and the figure shows area-weighted global averages. These satellite data have undergone extensive testing to identify errors and biases through comparison with independent satellite and ground-based profile observations, including the NOAA reference ozone network (Kramarova, Frith, et al., 2013).

9. Data Limitations

Factors that may impact the confidence, application, or conclusions drawn from this indicator are as follows:

1. This indicator does not track water vapor because of its spatial and temporal variability. Human activities have only a small direct impact on water vapor concentrations, but there are indications that increasing global temperatures are leading to increasing levels of atmospheric humidity (Dai et al., 2011).

2. Some radiatively important atmospheric constituents that are substantially affected by human activities (such as black carbon, aerosols, and sulfates) are not included in this indicator because of their spatial and temporal variability.

3. This indicator includes several of the most important halogenated gases, but some others are not shown. Many other halogenated gases are also GHGs, but Figure 4 is limited to a set of common examples that represent most of the major types of these gases.

4. Ice core measurements are not taken in real time, which introduces some error into the date of the sample. Dating accuracy for the ice cores ranges up to plus or minus 20 years (often less), depending on the method used and the time period of the sample. Diffusion of gases from the samples, which would tend to reduce the measured values, could also add a small amount of uncertainty.

5. Factors that could affect satellite-based ozone measurements include orbital drift, instrument differences, and solar zenith angle (the angle of incoming sunlight) at the time of measurement. As discussed in Section 10, however, the data have been filtered and calibrated to account for these factors. For example, Figure 5 has been restricted to the zone between 50°N and 50°S latitude because at higher latitudes the solar zenith angles would introduce greater uncertainty and because the lack of sunlight during winter months creates data gaps.

10. Sources of Uncertainty

Figures 1, 2, 3, and 4. Global Atmospheric Concentrations of Carbon Dioxide, Methane, Nitrous Oxide, and Selected Halogenated Gases

Direct measurements of atmospheric concentrations, which cover approximately the last 50 years, are of a known and high quality. Generally, standard errors and accuracy measurements are computed for the data.

For ice core measurements, uncertainties result from the actual gas measurements as well as the dating of each sample. Uncertainties associated with the measurements are believed to be relatively small, although diffusion of gases from the samples might also add to the measurement uncertainty. Dating accuracy for the ice cores is believed to be within plus or minus 20 years, depending on the method used and the time period of the sample. This level of uncertainty is insignificant, however, considering that some ice cores characterize atmospheric conditions for time frames of hundreds of thousands of years. The original scientific publications (see Section 3) provide more detailed information on the estimated uncertainty within the individual data sets.

Visit the Carbon Dioxide Information Analysis Center (CDIAC) archive (https://data.ess-dive.lbl.gov/portals/CDIAC) for more information on the accuracy of both direct and ice core measurements.

Overall, the concentration increase in GHGs in the past century is far greater than the estimated uncertainty of the underlying measurement methodologies. It is highly unlikely that the concentration trends depicted in this set of figures are artifacts of uncertainty.

Figure 5. Global Atmospheric Concentrations of Ozone, 1979–2020

NASA has estimated uncertainties for the merged SBUV satellite ozone data set, mostly focusing on errors that might affect trend analysis. Constant offsets and random errors will make no difference in the trend, but smoothing error and instrumental drift can potentially affect trend estimates. The following discussion describes these sources of error, the extent to which they affect the data used for this indicator, and steps taken to minimize the corresponding uncertainty.

- The main source of error in the SBUV data is a smoothing error due to profile variability that the SBUV observing system cannot inherently measure (Bhartia et al., 2012; Kramarova, Bhartia, et al., 2013). NASA's SBUV data set is divided into 21 distinct layers of the atmosphere, and the size of the smoothing error varies depending on the layer. For the layers that make up most of the stratosphere (specifically between 16 hectopascals [hPa] and 1 hPa of pressure in the tropics [20°S to 20°N] and 25 hPa to 1 hPa outside the tropics), the smoothing error for the SBUV monthly mean profiles is approximately 1 percent, indicating that SBUV data are capable of accurately representing ozone changes in this part of the atmosphere. For the SBUV layers that cover the troposphere, the lower stratosphere, and above the stratosphere (air pressure less than 1 hPa), the smoothing errors are larger: up to 8 to 15 percent. The influence of these smoothing errors has been minimized by adding all of the individual SBUV layers together to examine total column ozone.

- Long-term drift can only be estimated through comparison with independent data sources. NASA validated the SBUV merged ozone data set against independent satellite observations and found that drifts are less than 0.3 percent per year and mostly insignificant.

- Several SBUV instruments have been used over time, and each instrument has specific characteristics. NASA estimated the offsets between pairs of SBUV instruments when they overlap (Deland et al., 2012) and found that mean differences are within 7 percent, with corresponding standard deviations of 1 to 3 percent. The SBUV Version 8.6 algorithm adjusts for these differences based on a precise comparison of radiance measurements during overlap periods.

- Because the SBUV instruments use wavelengths that have high sensitivity to ozone, the total column ozone calculated from this method is estimated to have a 1 to 2 Dobson unit accuracy for solar zenith angles up to 70 degrees—i.e., when the sun is more than 20 degrees above the horizon (Bhartia et al., 2012). Measurements taken when the sun is lower in the sky have less accuracy, which is why the SBUV data in this indicator have been mostly limited to measurements made between 8 AM and 4 PM Equatorial Crossing Time, and one reason why the data have been limited to the area between 50°N and 50°S latitude (77 percent of the Earth's surface area).

Fishman et al. (2003) describe uncertainties in the TOR tropospheric ozone data set. Calculations of global average TOR may vary by up to 5 Dobson units, depending on which release of satellite data is used. For information about uncertainty in the OMI Level 2 tropospheric ozone data set, see Ziemke et al. (2006), which describes in detail how OMI data have been validated against ozonesonde data. Both of these data sets have been limited to the zone between 50°N and 50°S latitude because of the solar angle limitation described above. Based on the considerations, adjustment steps, and validation steps described above, it is unlikely that the patterns depicted in Figure 5 are artifacts of uncertainty.

11. Sources of Variability

Figures 1, 2, 3, and 4. Global Atmospheric Concentrations of Carbon Dioxide, Methane, Nitrous Oxide, and Selected Halogenated Gases

Atmospheric concentrations of the long-lived GHGs vary with both time and space. The data presented in this indicator, however, have extraordinary temporal coverage. For carbon dioxide, methane, and nitrous oxide, concentration data span several hundred thousand years; for the halogenated gases, data span virtually the entire period during which these largely synthetic gases were widely used. While spatial coverage of monitoring stations is more limited, most of the GHGs presented in this indicator are considered to be well-mixed globally, due in large part to their long residence times in the atmosphere.

Figure 5. Global Atmospheric Concentrations of Ozone, 1979–2020

Unlike the other gases described in this indicator, ozone is relatively short-lived in the troposphere, with a typical lifetime of only a few weeks. Concentrations of both tropospheric and stratospheric ozone vary spatially at any given time; for example, Fishman et al. (2003) use the TOR to show noticeably elevated levels of tropospheric ozone over heavily populated and industrialized regions. Fishman et al. (2003) also show seasonal variations. This indicator accounts for both spatial and temporal variations by presenting global annual averages.

12. Statistical/Trend Analysis

This indicator presents a time series of atmospheric concentrations of GHGs. For the long-lived gases, no statistical techniques or analyses have been used here to characterize the long-term trends or their statistical significance. The latest authoritative scientific assessments have concluded that concentrations of these gases substantially exceed the highest concentrations recorded in ice cores during the past 800,000 years (IPCC, 2021).

For ozone, EPA used ordinary least-squares linear regressions as a screening-level assessment of whether changes in ozone levels over time have been statistically significant. This analysis yielded the following results:

- A regression of the total column ozone data from 1979 to 2020 shows a significant decrease of approximately 0.16 Dobson units per year ($p < 0.001$).
- Further analysis of the total column ozone data shows a rapid decline over the first decade and a half of the data record (1979–1994), with insignificant change after that. A regression analysis for 1979–1994 shows a significant decline of about 0.74 Dobson units per year ($p < 0.001$), while the regression for the remainder of the data record (1995-2020) shows an insignificant change ($p = 0.34$).
- A regression of tropospheric ozone from 1979 to 2020 shows a significant increase of 0.10 Dobson units per year ($p < 0.001$).

References

AGAGE (Advanced Global Atmospheric Gases Experiment). (2011). *Data provided to ERG (an EPA contractor) by Ray Wang, Georgia Institute of Technology* (November 2011.) [Data set].

AGAGE (Advanced Global Atmospheric Gases Experiment). (2021). *ALE/GAGE/AGAGE database* (updated June 21, 2021) [Data set]. Retrieved March 1, 2024, from https://agage.eas.gatech.edu/data_archive/global_mean/global_mean_md.txt

AGAGE (Advanced Global Atmospheric Gases Experiment). (2022). *ALE/GAGE/AGAGE database* (updated June 14, 2022) [Data set]. Retrieved March 1, 2024, from https://agage2.eas.gatech.edu/data_archive/global_mean

Arnold, T., Harth, C. M., Mühle, J., Manning, A. J., Salameh, P. K., Kim, J., Ivy, D. J., Steele, L. P., Petrenko, V. V., Severinghaus, J. P., Baggenstos, D., & Weiss, R. F. (2013). Nitrogen trifluoride global emissions estimated from updated atmospheric measurements. *Proceedings of the National Academy of Sciences*, *110*(6), 2029–2034. https://doi.org/10.1073/pnas.1212346110

Arnold, T., Mühle, J., Salameh, P. K., Harth, C. M., Ivy, D. J., & Weiss, R. F. (2012). Automated measurement of nitrogen trifluoride in ambient air. *Analytical Chemistry*, *84*(11), 4798–4804. https://doi.org/10.1021/ac300373e

Battle, M., Bender, M., Sowers, T., Tans, P. P., Butler, J. H., Elkins, J. W., Ellis, J. T., Conway, T., Zhang, N., Lang, P., & Clarket, A. D. (1996). Atmospheric gas concentrations over the past century measured in air from firn at the South Pole. *Nature*, *383*(6597), 231–235. https://doi.org/10.1038/383231a0

Bereiter, B., Eggleston, S., Schmitt, J., Nehrbass-Ahles, C., Stocker, T. F., Fischer, H., Kipfstuhl, S., & Chappellaz, J. (2015). Revision of the EPICA Dome C CO_2 record from 800 to 600 kyr before present. *Geophysical Research Letters*, *42*(2), 542–549. https://doi.org/10.1002/2014GL061957

Bhartia, P. K., McPeters, R. D., Flynn, L. E., Taylor, S., Kramarova, N. A., Frith, S., Fisher, B., & Deland, M. (2012). Solar Backscatter UV (SBUV) total ozone and profile algorithm. *Atmospheric Measurement Techniques Discussions*, *5*, 5913–5951. https://doi.org/10.5194/amtd-5-5913-2012

Chamard, P., Ciattaglia, L., di Sarra, A., & Monteleone, F. (2001). Atmospheric carbon dioxide record from flask measurements at Lampedusa Island. In *Trends: A compendium of data on global change*. U.S. Department of Energy. https://cdiac.ess-dive.lbl.gov/trends/co2/lampis.html

CSIRO (Commonwealth Scientific and Industrial Research Organisation). (2024a). *Monthly mean baseline (background) carbon dioxide concentrations measured at the Cape Grim Baseline Air Pollution Station, Tasmania, Australia* (updated January 2024) [Data set]. Retrieved March 4, 2024, from http://capegrim.csiro.au/GreenhouseGas/data/CapeGrim_CO2_data_download.csv

CSIRO (Commonwealth Scientific and Industrial Research Organisation). (2024b). *Monthly mean baseline (background) methane concentrations measured at the Cape Grim Baseline Air Pollution Station, Tasmania, Australia* (updated January 2024) [Data set]. Retrieved March 5, 2024, from http://capegrim.csiro.au/GreenhouseGas/data/CapeGrim_CH4_data_download.csv

CSIRO (Commonwealth Scientific and Industrial Research Organisation). (2024c). *Monthly mean baseline (background) nitrous oxide concentrations measured at the Cape Grim Baseline Air Pollution Station, Tasmania, Australia* (updated January 2024) [Data set]. Retrieved March 11, 2024, from http://capegrim.csiro.au/GreenhouseGas/data/CapeGrim_N2O_data_download.csv

Dai, A., Wang, J., Thorne, P. W., Parker, D. E., Haimberger, L., & Wang, X. L. (2011). A new approach to homogenize daily radiosonde humidity data. *Journal of Climate*, *24*(4), 965–991. https://doi.org/10.1175/2010JCLI3816.1

Deland, M. T., Taylor, S. L., Huang, L.-K., & Fisher, B. L. (2012). Calibration of the SBUV version 8.6 ozone data product. *Atmospheric Measurement Techniques Discussions*, *5*, 5151–5203. https://doi.org/10.5194/amtd-5-5151-2012

Etheridge, D. M., Steele, L. P., Francey, R. J., & Langenfelds, R. L. (2002). Historic CH_4 records from Antarctic and Greenland ice cores, Antarctic firn data, and archived air samples from Cape Grim, Tasmania. In *Trends: A compendium of data on global change*. U.S. Department of Energy. http://cdiac.ess-dive.lbl.gov/trends/atm_meth/lawdome_meth.html

Fishman, J., Wozniak, A. E., & Creilson, J. K. (2003). Global distribution of tropospheric ozone from satellite measurements using the empirically corrected tropospheric ozone residual technique: Identification of the regional aspects of air pollution. *Atmospheric Chemistry and Physics*, *3*(4), 893–907. https://doi.org/10.5194/acp-3-893-2003

IPCC (Intergovernmental Panel on Climate Change). (2013). *Climate change 2013—The physical science basis: Contribution of Working Group I to the Fifth Assessment Report of the Intergovernmental Panel on Climate Change* (T. F. Stocker, D. Qin, G.-K. Plattner, M. Tignor, S. K. Allen, A. Boschung, A. Nauels, Y. Xia, V. Bex, & Midgley, Eds.). Cambridge University Press. www.ipcc.ch/report/ar5/wg1

IPCC (Intergovernmental Panel on Climate Change). (2021). Summary for policymakers. In *Climate change 2021: The physical science basis. Working Group I contribution to the IPCC Sixth Assessment Report*. Cambridge University Press. www.ipcc.ch/assessment-report/ar6

Kramarova, N. A., Bhartia, P. K., Frith, S. M., McPeters, R. D., & Stolarski, R. S. (2013). Interpreting SBUV smoothing errors: An example using the quasi-biennial oscillation. *Atmospheric Measurement Techniques*, *6*(8), 2089–2099. https://doi.org/10.5194/amt-6-2089-2013

Kramarova, N. A., Frith, S. M., Bhartia, P. K., McPeters, R. D., Taylor, S. L., Fisher, B. L., Labow, G. J., & DeLand, M. T. (2013). Validation of ozone monthly zonal mean profiles obtained from the version 8.6 Solar Backscatter Ultraviolet algorithm. *Atmospheric Chemistry and Physics*, *13*(14), 6887–6905. https://doi.org/10.5194/acp-13-6887-2013

Labow, G. J., McPeters, R. D., Bhartia, P. K., & Kramarova, N. (2013). A comparison of 40 years of SBUV measurements of column ozone with data from the Dobson/Brewer network. *Journal of Geophysical Research: Atmospheres*, *118*(13), 7370–7378. https://doi.org/10.1002/jgrd.50503

Loulergue, L., Schilt, A., Spahni, R., Masson-Delmotte, V., Blunier, T., Lemieux, B., Barnola, J.-M., Raynaud, D., Stocker, T. F., & Chappellaz, J. (2008). Orbital and millennial-scale features of atmospheric CH_4 over the past 800,000 years. *Nature*, *453*(7193), 383–386. https://doi.org/10.1038/nature06950

McPeters, R. D., Bhartia, P. K., Haffner, D., Labow, G. J., & Flynn, L. (2013). The version 8.6 SBUV ozone data record: An overview. *Journal of Geophysical Research: Atmospheres*, *118*(14), 8032–8039. https://doi.org/10.1002/jgrd.50597

NASA (National Aeronautics and Space Administration). (2013). *Data—TOMS/SBUV TOR data products* [Data set]. Retrieved November 1, 2013, from https://science-data.larc.nasa.gov/TOR/data.html

NASA (National Aeronautics and Space Administration). (2021). *Tropospheric ozone data from AURA OMI/MLS* [Data set]. Retrieved May 1, 2022, from https://acd-ext.gsfc.nasa.gov/Data_services/cloud_slice/new_data.html

NASA (National Aeronautics and Space Administration). (2022). *SBUV merged ozone data set (MOD)* (Version 8.7, updated May 21, 2022) [Data set]. Retrieved March 1, 2024, from https://acdb-ext.gsfc.nasa.gov/Data_services/merged/index.html

NOAA (National Oceanic and Atmospheric Administration). (2023a). *Halocarbons and other Atmospheric Trace Species (HATS) group* (updated October 2023) [Data set]. Retrieved March 1, 2024, from https://gml.noaa.gov/aftp/data/hats/Total_Cl_Br

NOAA (National Oceanic and Atmospheric Administration). (2023b). *Monthly mean CH_4 concentrations for Mauna Loa, Hawai'i* (updated August 28, 2023) [Data set]. Retrieved March 5, 2024, from https://gml.noaa.gov/aftp/data/trace_gases/ch4/flask/surface

NOAA (National Oceanic and Atmospheric Administration). (2023c). *Monthly mean N_2O concentrations for Mauna Loa, Hawai'i* (updated August 29, 2023) [Data set]. Retrieved March 11, 2024, from www.esrl.noaa.gov/gmd/hats/insitu/cats/cats_conc.html

NOAA (National Oceanic and Atmospheric Administration). (2024a). *Annual mean carbon dioxide concentrations for Mauna Loa, Hawai'i* (updated March 5, 2024) [Data set]. Retrieved March 5, 2024, from https://gml.noaa.gov/ccgg/trends/data.html

NOAA (National Oceanic and Atmospheric Administration). (2024b). *Monthly mean carbon dioxide concentrations for Barrow, Alaska; Cape Matatula, American Samoa; and the South Pole* (updated February 12, 2024) [Data set]. Retrieved March 5, 2024, from https://gml.noaa.gov/aftp/data/trace_gases/co2/in-situ/surface

NOAA (National Oceanic and Atmospheric Administration). (2024c). *Monthly mean N_2O concentrations for Barrow, Alaska, and the South Pole* (updated February 9, 2024) [Data set]. Retrieved March 11, 2024, from www.esrl.noaa.gov/gmd/hats/insitu/cats/cats_conc.html

Rigby, M. (2017). Update to data originally published in: Arnold, T., Harth, C. M., Mühle, J., Manning, A. J., Salameh, P. K., Kim, J., Ivy, D. J., Steele, L. P., Petrenko, V. V., Severinghaus, J. P., Baggenstos, D., & Weiss, R. F. (2013). Nitrogen trifluoride global emissions estimated from updated atmospheric measurements. *Proceedings of the National Academy of Sciences of the United States of America*, *110*(6), 2029–2034. https://doi.org/10.1073/pnas.1212346110

Schilt, A., Baumgartner, M., Blunier, T., Schwander, J., Spahni, R., Fischer, H., & Stocker, T. F. (2010). Glacial–interglacial and millennial-scale variations in the atmospheric nitrous oxide concentration during the last 800,000 years. *Quaternary Science Reviews*, *29*(1–2), 182–192. https://doi.org/10.1016/j.quascirev.2009.03.011

Steele, L. P., Krummel, P. B., & Langenfelds, R. L. (2002). Atmospheric methane record from Shetland Islands, Scotland (October 2002 version). In *Trends: A compendium of data on global change*. U.S. Department of Energy. https://cdiac.ess-dive.lbl.gov/trends/atm_meth/csiro/csiro-shetlandch4.html

Steele, L. P., Krummel, P. B., & Langenfelds, R. L. (2007). *Atmospheric CO_2 concentrations (ppmv) derived from flask air samples collected at Cape Grim, Australia, and Shetland Islands, Scotland* [Data set]. Commonwealth Scientific and Industrial Research Organisation. Retrieved January 20, 2009, from https://cdiac.ess-dive.lbl.gov/trends/co2/csiro

Weiss, R. F., Mühle, J., Salameh, P. K., & Harth, C. M. (2008). Nitrogen trifluoride in the global atmosphere. *Geophysical Research Letters*, *35*(20), L20821. https://doi.org/10.1029/2008GL035913

Ziemke, J. R., Chandra, S., Duncan, B. N., Froidevaux, L., Bhartia, P. K., Levelt, P. F., & Waters, J. W. (2006). Tropospheric ozone determined from Aura OMI and MLS: Evaluation of measurements and comparison with the Global Modeling Initiative's Chemical Transport Model. *Journal of Geophysical Research: Atmospheres*, *111*(D19), 2006JD007089. https://doi.org/10.1029/2006JD007089